

Figure S1: *Clec4f^{ΔComm10}* KCs fit into the KC niche, but are being replaced by MoKCs; related to Figure 1. (A) Representative flow cytometry images displaying gating strategy used to define KCs and infiltrating Ly6C^{hi} monocytes and neutrophils in the healthy liver. (B-D) Representative confocal microscopy images obtained from liver sections of *Comm10^{fl/fl}* and *Clec4f^{ΔComm10}*. (B) Expression of Clec4F (red), F4/80 (green) and nuclei (blue), original magnification: $\times 20$. Bars= 100 μ m. (C) Expression of Clec4F (red) and desmin (yellow), original magnification: $\times 40$. Bars=200 μ m. (D) Expression of Clec4F (red) and desmin (yellow), CD31 (cyan) and nuclei (blue). Original magnification: $\times 20$. Bars= 100 μ m. (E) Representative flow cytometry plots displaying the representation of CD163⁻ and VSIG4⁻ among *Comm10^{fl/fl}* and *Clec4f^{ΔComm10}* KCs. (F) Left, mean fluorescence intensity (MFI) of CLEC4F. Right, representative histogram plot showing expression of CLEC4F on *Comm10^{fl/fl}* and *Cx3cr1^{ΔComm10}* KCs, in comparison to isotype control (dashed black line) (n=3). (G-I) mean fluorescence intensity (MFI) of TIM4 expression in KCs from (G) perinatal mice, (H), eight weeks old mice, and (I) intracellular staining of TIM4 in KCs. (G-I: n \geq 3) (J) Frequency of TIM4⁺ cells among KCs from eight and 24-30 weeks old *Comm10^{fl/fl}* and *Cx3cr1^{ΔComm10}* mice (n>5). (K) Representative flow cytometry plots showing depletion of KC following clodronate liposome treatment. Data were analyzed by unpaired, two-tailed *t*-test and are presented as mean \pm SEM with significance: ****p* < 0.001. Experiments were repeated at least 3 times (A-F), twice (H, J) or once (G, I, K).

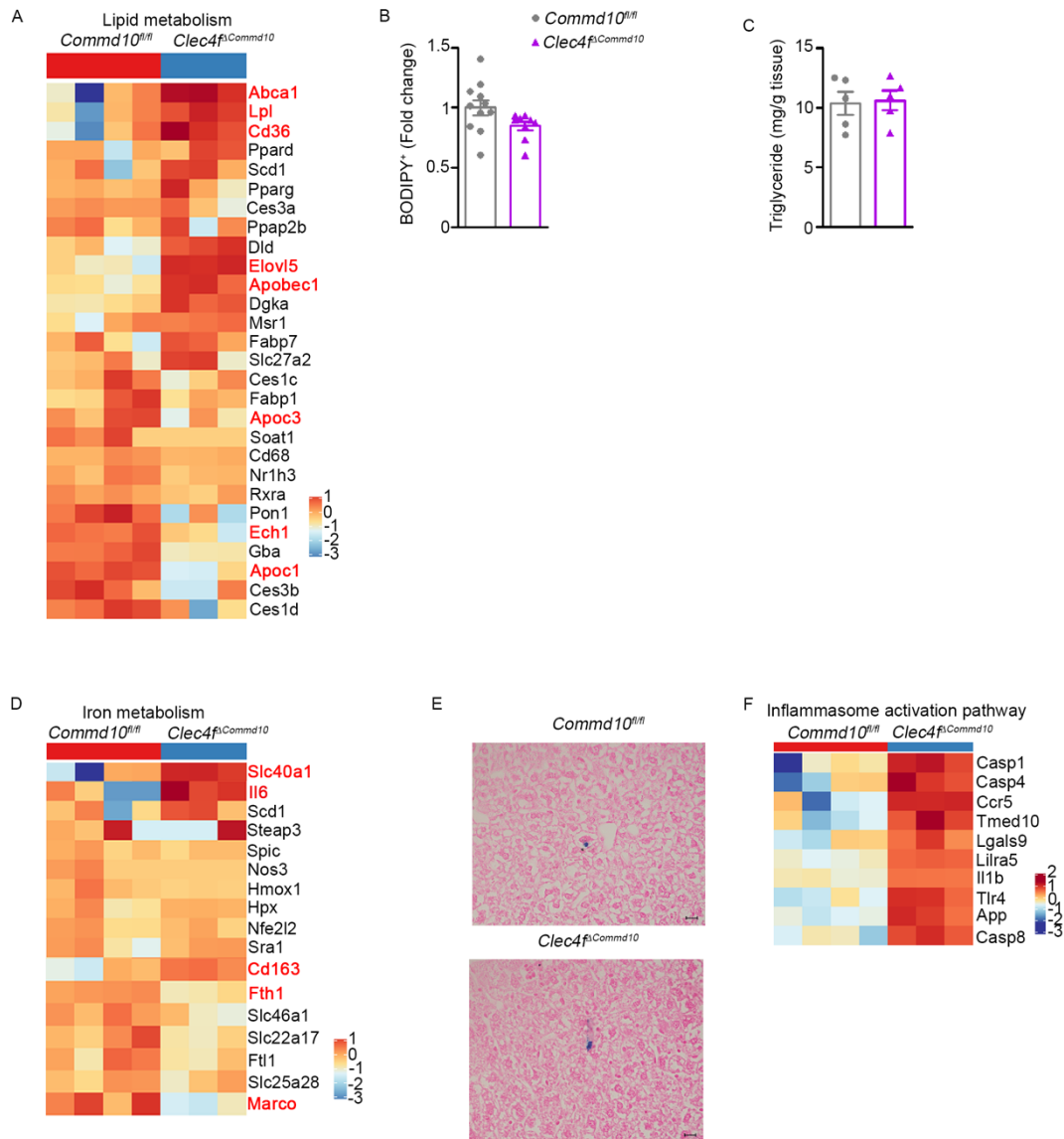


Figure S2: COMMD10-deficient KCs acquire liver-specific functional KC identity; related to Figure 2.

(A) MARS-RNAseq heat map analysis displaying expression of genes associated with lipid metabolism in *Commmd10^{fl/fl}* versus *Clec4^{ΔCommmd10}* KCs. (B) Neutral lipid content of *Commmd10^{fl/fl}* and *Clec4^{ΔCommmd10}* steady state KCs. Results shown are mean fluorescence intensity (MFI) for BODIPY staining (n>10). (C) Triglycerides levels normalized to liver tissue mass in *Commmd10^{fl/fl}* and *Clec4^{ΔCommmd10}* livers (n=5). (D) MARS-RNAseq heat map analysis displaying expression of genes associated with iron metabolism in *Commmd10^{fl/fl}* versus *Clec4^{ΔCommmd10}* KCs. (E) Representative images of Perl's iron, with Prussian blue reaction staining of *Commmd10^{fl/fl}* and *Clec4^{ΔCommmd10}* liver sections. Original magnification= x4. Bars=50μm. (F) MARS-RNAseq heat map analysis of *Commmd10^{fl/fl}* versus *Clec4^{ΔCommmd10}* KCs displaying variance of genes associated with inflammasome activation pathway. For A and D, significantly differentially expressed genes are marked red. Analysis was performed on differentially expressed genes (n>3, $p < 0.05$; raw P values were adjusted for multiple testing using the procedure of Benjamini and Hochberg, ≥ 1.5 -fold change).

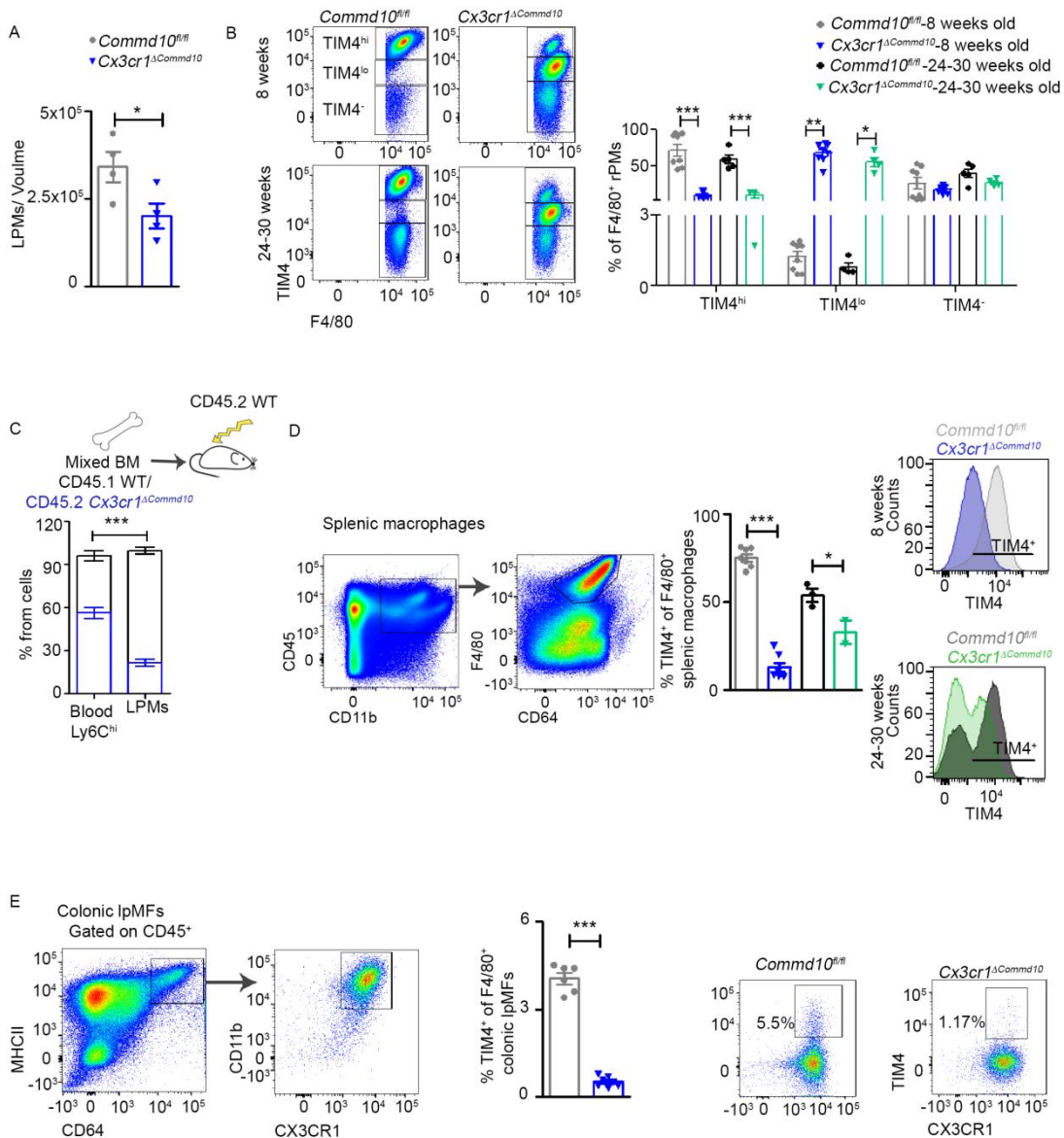


Figure S3: COMMD10 is crucial for the homeostatic maintenance of resident macrophages of the peritoneum, spleen and gut; related to Figure 3.

(A) LPMs counts normalized to extracted volume of peritoneal lavage in *Commd10^{fl/fl}* and *Cx3cr1^{ΔCommd10}* mice (n=4). (B) Quantification of TIM4⁺, TIM4^{lo} and TIM4⁻ LPMs frequency among total LPMs from *Commd10^{fl/fl}* and *Cx3cr1^{ΔCommd10}* mice (n≥4). (C) quantification of % chimerism in blood Ly6C^{hi} monocytes and LPMs assessed in mixed CD45.1 WT/ CD45.2 *Cx3cr1^{ΔCommd10}* BM chimeras at eight weeks post irradiation (n≥8). (D) Left, frequency of TIM4⁺ among splenic macrophages in eight versus 24-30 weeks old *Commd10^{fl/fl}* and *Cx3cr1^{ΔCommd10}* mice. Right, representative histogram plot showing expression level of TIM4. (E) Left, frequency of TIM4⁺ among colonic lamina propria macrophages (IpMFs) in eight weeks old *Commd10^{fl/fl}* and *Cx3cr1^{ΔCommd10}* mice. Right, representative flow cytometry plot showing expression level of TIM4 in IpMFs (24-30 weeks: n>2, eight weeks n=4). Data were analyzed by unpaired, two-tailed *t*-test and are presented as mean ± SEM with significance: **p* < 0.05, ***p* < 0.01, ****p* < 0.001. Experiments were repeated twice (B, C, D, E) or once (A).

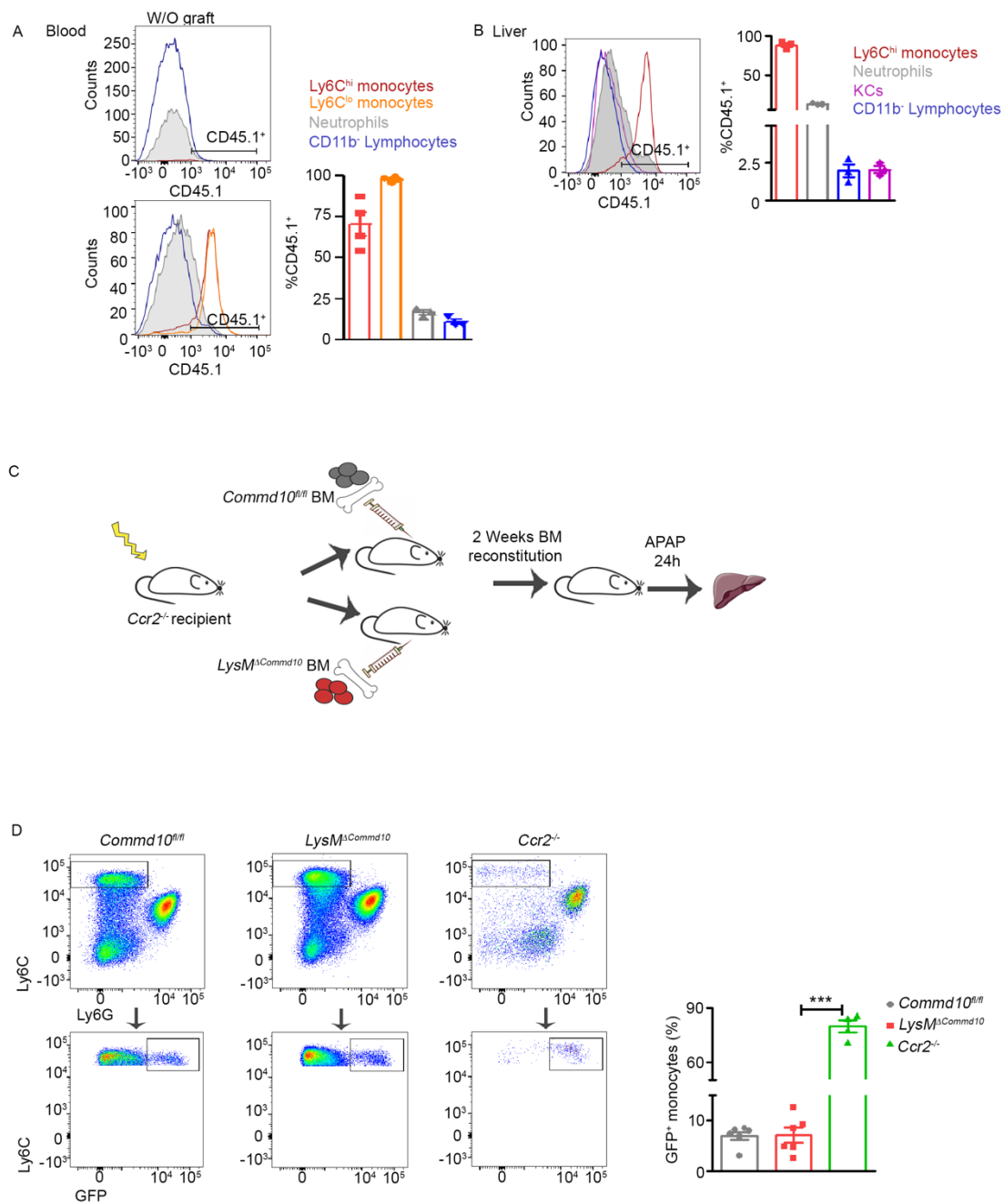


Figure S4: COMMD10 is important for tuning the inflammatory activity of Ly6C^{hi} monocytes in acetaminophen-induced liver injury (AILI); related to Figure 5. Irradiated (3 Gy) *Cx3cr1^{gfp/+}Ccr2^{-/-}* mice were engrafted with CD45.1 congenic BM, allowed to reconstitute for two weeks, and then subjected to AILI 24 h (n>4). (A- B) Representative flow cytometry images illustrating the chimerism (% of CD45.1⁺) obtained in (A) blood and (B) liver in indicated immune cells. (C) Schematic illustration of the experimental design: irradiated (3 Gy) *Cx3cr1^{gfp/+}Ccr2^{-/-}* mice were engrafted with BM from *LysM^{ΔComm10}* or *Comm10^{fl/fl}* littermate mice. Two weeks post reconstitution, mice were subjected to AILI 24 h. (D) Representative flow cytometry images illustrating the chimerism obtained in liver Ly6C^{hi} monocytes marked by their negative expression of CX3CR1-GFP reporter protein. Data were analyzed by unpaired, two-tailed t-test and are presented as mean ± SEM with significance: ***p< 0.001. Data are representative three independent experiments.

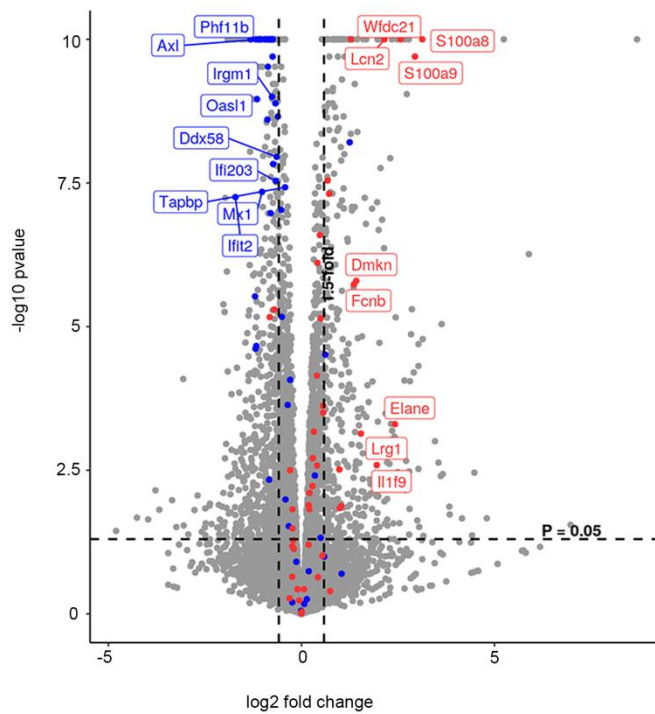


Figure S5: COMMD10-deficient Ly6C^{hi} monocytes display higher expression of ‘neutrophil-like’ monocyte (NeuMo) signature genes; related to Figure 6. Volcano plots comparing *Commd10*^{fl/fl} and *LysM*^{Cre}*Commd10*^{fl/fl} Ly6C^{hi} monocytes, the expression pattern of both NeuMo and DCMo associated genes as depicted from (Weinreb et al., 2020). Analysis was performed on differentially expressed genes ($n > 3$, $p < 0.05$; raw P values were adjusted for multiple testing using the procedure of Benjamini and Hochberg, ≥ 1.5 -fold change).

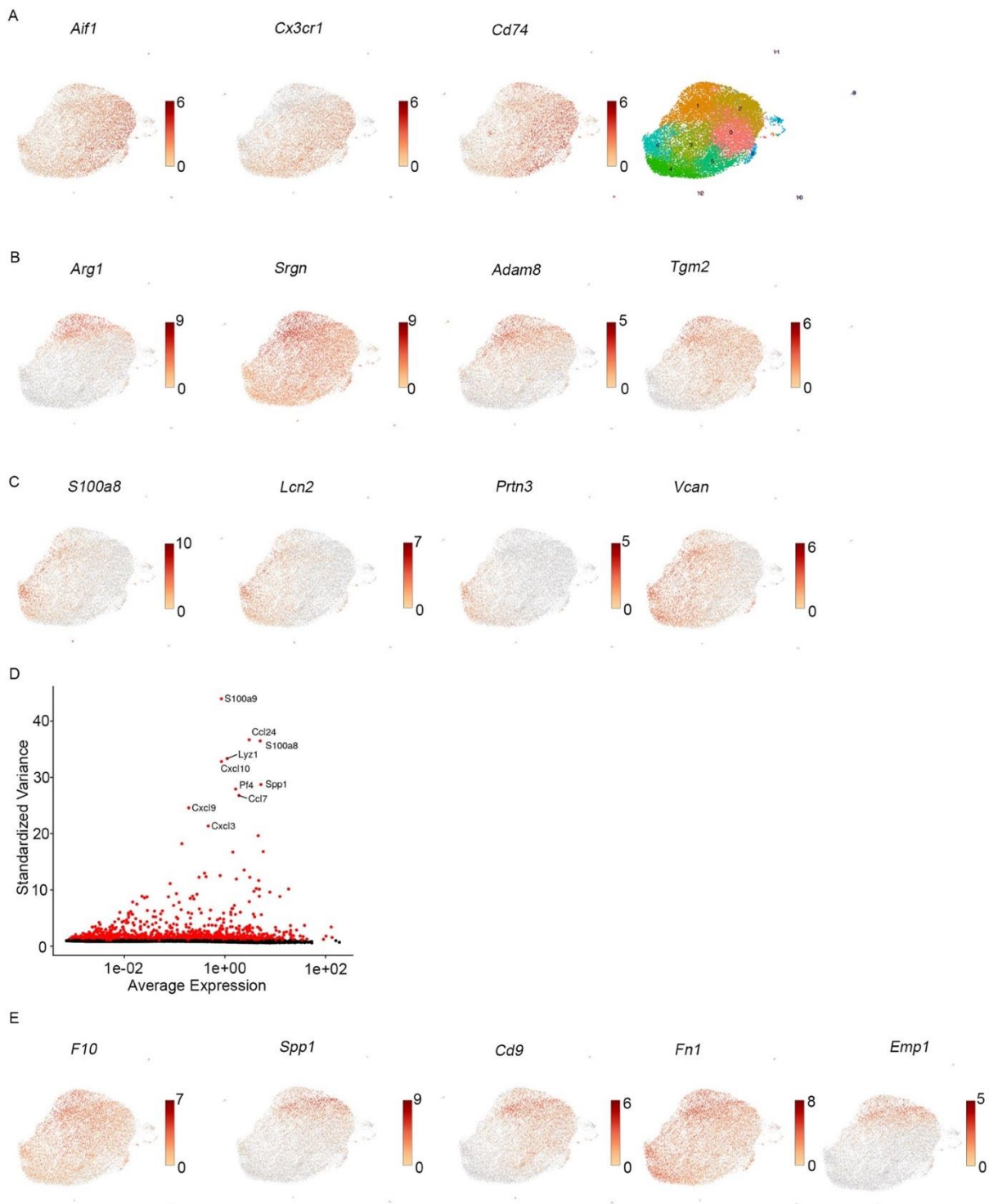


Figure S6: COMMD10 deletion-induces a biased differentiation of $Ly6C^{hi}$ monocytes toward ‘neutrophil-like’ monocytes (NeuMo) and lipid associated macrophages (LAMs); related to Figure 7. Single cell RNA-seq analysis of liver $Ly6C^{hi}$ monocytes at AILI 24 h. Gene expression domains of (A) cluster 0, (B) cluster 1, (C) NeoMo markers (D) and (E) LAM markers. Analysis was performed on differentially expressed genes ($p < 0.05$; non-parametric Wilcoxon rank sum test, ≥ 1.5 -fold change).

REAGENT or RESOURCE	SOURCE	IDENTIFIER
<i>Tnfa</i> FWD:GGTGCCTATGTCTCAGCCTCTT	Merck	N/A
<i>Tnfa</i> REV:GCCATAGAAGCTGATGAGAGGGAG	Merck	N/A
<i>Il-1b</i> FWD:TGGACCTTCCAGGATGAGGACA	Merck	N/A
<i>Il-1b</i> REV: GTTCATCTCGGAGCCTGTAGTG	Merck	N/A
<i>Cxcl1</i> FWD:TCCAGAGCTTGAAGGTGTTGCC	Merck	N/A
<i>Cxcl1</i> REV:AACCAAGGGAGCTTCAGGGTCA	Merck	N/A
<i>Cxcl2</i> FWD: CATCCAGAGCTTGAGTGTGACG	Merck	N/A
<i>Cxcl2</i> REV: GGCTTCAGGGTCAAGGCAAAGT	Merck	N/A
<i>Timd4</i> FWD: CTACAGACAAGCCGTAAGTCA	Merck	N/A
<i>Timd4</i> REV: GTCTTCATCATCCCTCCC	Merck	N/A
<i>Ccl1</i> FWD: GCTACAAGAGGATCACCAGCAG	Merck	N/A
<i>Ccl2</i> REV: GTCTGGACCCATTCCTTCTTGG	Merck	N/A
<i>Gata6</i> FWD:ATGCGGTCTACAGCAAGATGA	Merck	N/A
<i>Gata6</i> REV: CGCCATAAGGTAGTGGTTGTGG	Merck	N/A

Figure S7: List of oligonucleotide sequences used for qRT-PCR; Related to Figure 1F, Figure 3B, Figure 4F, Figure 5E.